Reduction of Threading Dislocation Density beyond the saturation limit by optimized reverse grading

Oliver Skibitzki[1,*], Marvin H. Zoellner[1], Fabrizio Rovaris[2], Markus Andreas Schubert[1], Yuji Yamamoto[1,] Luca Persichetti[3], Luciana Di Gaspare[3], Monica De Seta[3], Riccardo Gatti[4], Francesco Montalenti[2], and Giovanni Capellini[1,3]

[1] *IHP - Leibniz-Institut für innovative Mikroelektronik, Im Technologiepark 25, 15236 Frankfurt (Oder), Germany*

[2] *L-NESS and Department of Materials Science, Università di Milano-Bicocca, Via Cozzi 55, I-20125, Milano, Italy*

[3] *Dipartimento di Scienze, Università Roma Tre, viale G. Marconi 446, Roma I-00146, Italy*

[4] *LEM, CNRS–ONERA, 29 Avenue de la Division Leclerc, BP 72, 92322 Châtillon Cedex, France*

KEYWORDS

Virtual substrate, Reverse-graded buffers, Germanium, Silicon, Threading dislocations, Heterointerfaces, Defect simulation, Reduced pressure chemical vapor deposition.

Corresponding authors

* Email: skibitzki@ihp-microelectronics.com

ABSTRACT

The threading dislocation density (TDD) in plastically relaxed Ge/Si(001) heteroepitaxial films is commonly observed to progressively decrease with their thickness, owing to mutual annihilation. However, there exists a saturation limit, known as the geometrical limit, beyond which a further decrease of the TDD in the Ge film is hindered. Here, we show that such limit can be overcome in SiGe/Ge/Si heterostructures thanks to the beneficial role of the second interface. Indeed, we show that $Si_{0.06}Ge_{0.94}$/Ge/Si(001) films display a TDD remarkably lower than the saturation limit of Ge/Si(001). Such result is interpreted with the help of Dislocation Dynamics simulations. The reduction of TDD is attributed to the enhanced mobility acquired by pre-existing threading dislocations after bending at the new interface to release the strain in the upper layer.

Importantly, we demonstrate that the low TDD achieved in $Si_{0.06}Ge_{0.94}$/Ge/Si layers is preserved also when a second, relaxed Ge layer is subsequently deposited. This makes the present reverse-grading technique of direct interest also for achieving a low TDD in pure-Ge films.

I. INTRODUCTION

The epitaxial growth of high-germanium (Ge) content silicon-germanium ($Si_{1-x}Ge_x$) layers [$x > 0.7$] on silicon (Si) is still attracting a growing attention in the scientific community, owing to its potential impact on several technological applications in the field of photonic and electronic devices [1]. Only to name of few, we can cite the fabrication of pMOS fin field-effect transistors (FinFETs) based on highly strained Ge [2, 3]; the use of GeSi/Ge/Si as material for near-infrared integrated light sources [4, 5], photodetectors [6, 7], and optical modulators in the integrated silicon photonic platform [8, 9]; the role of high quality Ge/GeSi quantum wells in the realization of a semiconductor based qbits platform [10, 11]; and finally, as active material for the fabrication of a Si-based THz quantum cascade laser (QCL), which might provide an electrically pumped compact source of coherent THz radiation at room temperature [12, 13].

However, the heteroepitaxial growth of Ge-rich $Si_{1-x}Ge_x$ layers directly on Si is challenging, due to the large lattice mismatch in the 3 – 4% range [5]. Because of this large mismatch, the critical thickness for plastic relaxation of the heteroepitaxial strain is limited to a few nm only. After this threshold, 60 degree dislocation loops are nucleated, gliding on {111} planes and eventually dropping strain-relieving misfit segments at the heterointerface [14, 15], which are then bounded by the screw-type arms of the threading dislocations (TDs) [16].

Two different approaches have been commonly proposed in literature to achieve Ge or Ge-rich $Si_{1-x}Ge_x$ layers on Si. The first consists in relying on compositionally graded $Si_{1-x}Ge_x$ thick buffers as virtual substrates (VSs), where the Ge content is gradually increased to accommodate the elastic energy by means of a progressive plastic relaxation, thus promoting less entangled dislocation networks [17]. Furthermore, the persistence of a strained upper region during the growth of the layer provides a steady driving force for the motion of TDs, favoring their interaction and

annihilation [18]. This method, despite being widely reported for low [x < 0.5] Ge content [5], is unpractical to achieve with standard deposition techniques (such as reduced pressure chemical vapor deposition (RPCVD) or molecular beam epitaxy (MBE)) for Ge or Ge-rich $Si_{1-x}Ge_x$, due to the large buffer thickness (up to 20 µm [5, 19]) needed to reach the final composition range and to the resulting high surface roughness, requiring a chemical mechanical polishing process step for any practical application [2, 5].

Alternatively, a decade ago, it has been proposed to first deposit high quality Ge-rich $Si_{1-x}Ge_x$ layers on Si, by using Ge/Si(001) VSs followed by the deposition of *tensile* strained layers featuring a *decreasing* Ge content [2, 5, 20]. In this method, known as reverse-graded (RG)-VS, the deposition of a relaxed Ge film on Si is followed by a $Si_{1-x}Ge_x$ buffer growth with either an abrupt or reverse grading layer, being thick enough to relax the existing tensile strain. In this case, the excess strain built up in the RG layer during its deposition provides the additional mobility to the TDs, again leading to their eventual interaction and annihilation. Compared to the aforementioned forward graded thick VS approach, this RG method produces consistently smoother buffer layers with low root-mean-square (rms) roughness and low TD density (TDD). Shah *et al.*, for instance, compared both methods for achieving a $Si_{0.22}Ge_{0.78}$ VS on Si(001). The results showed that, for obtaining a $Si_{0.22}Ge_{0.78}$ VS with a TDD in the 10^6 cm^{-2} range, the RG method required a significantly thinner heterostructure (2.8 µm instead of ~ 8 µm), exhibiting also a six times smaller rms roughness (2.6 nm instead of ~ 15 nm) [21].

Clearly, the goal is to reduce the TDD to the lowest possible value, since TDs are responsible for the degeneration of the structural and consequently electrical and optical properties of the material.

In this paper, by using an industry-grade RPCVD system hosted in a fabrication pilot line, we performed a systematic investigation of the growth of $Si_{1-x}Ge_x$/Ge/Si(001) RG-VSs. As a relevant case study, the Ge content in the $Si_{1-x}Ge_x$ layer was fixed at x = 0.94, since this is the typical RG-VS compositional range required to realize a strain-balanced Si-based THz QCL heterostructure [12, 22]. All the samples were thoroughly analyzed in terms of their crystal defects (Misfit dislocations (MDs) and TDDs) and lattice properties (strain, composition profile, surface morphology). A close comparison between experimental results and theoretical Dislocation Dynamics (DD) simulations was carried out, allowing us to describe and understand the relaxation behavior as well as the dislocation propagation and annihilation during RG-VS growth. The main goals of this study were *i*) to understand the defect development and strain-release in $Si_{0.06}Ge_{0.94}$/Ge/Si(001) RG-VS and *ii*) to optimize the growth processes leading to the minimum TDD in RG-VSs, as a key milestone for the potential subsequent deposition of high-quality strain-compensated THz QCL structure on a Si platform.

II. EXPERIMENTAL AND SIMULATION METHODS

All the samples of this study were deposited on 200 mm Si(001) wafer in a commercial ASM Epsilon 2000 lamp-heated single wafer RPCVD reactor at a pressure of 80 Torr. Prior to the epitaxial growth, Si(001) substrates were wet chemically cleaned by a Radio Corporation of America solution, followed by a prebake in the chamber at 1000°C in hydrogen (H_2) atmosphere. For all samples, a 100 nm seed layer deposition Ge was grown at 350°C using germane (GeH_4) and nitrogen (N_2) as carrier gas. After the seed layer formation, variable thickness Ge layers were grown at a temperature of 550°C, using H_2 and GeH_4 as carrier and reactant gas, respectively. All the Ge substrate underwent a cyclic growth and annealing procedure for the Ge buffer layer, consisting of two annealing steps at 800°C. It is worth noting that this procedure leads to a reduction of the TDD by two order of magnitude, as

compared to the as-grown case [2, 23]. As described in the following, we have also realized two sample series in which $Si_{0.06}Ge_{0.94}$ layers, with a thickness up to 1.2 μm, were grown on top of Ge/Si layers at 550°C, using silane (SiH_4) and GeH_4 as reactant gas.

X-ray diffraction (XRD) measurements were performed using a Rigaku SmartLab diffractometer equipped with a 9 kW rotating Cu anode (Cu K_α = 0.1541 nm). In-plane and out-of-plane lattice constants were determined analyzing the (004) and (224) Bragg reflections. The unstrained lattice constant was derived by assuming a tetragonal distortion of the lattice and a Poisson ratio corresponding to the nominal stoichiometry. Finally, the stoichiometry was determined by taking into account the deviation from Vegards law published by Dismukes *et al*. [24].

The surface morphology was studied by a Bruker Dimension Icon atomic force microscope (AFM), working in PeakForce Tapping mode while the structural quality was investigated by (scanning) transmission electron microscopy ((S)TEM) using a FEI Tecnai Osiris operating at 200 kV. TEM lamellas were prepared by milling and undercutting processes using a Zeiss NVision 40 focused ion beam operating at up to 30 kV.

We performed the TDD analysis relying on a defect decoration method (etch pit count). The defect decoration was achieved using a calibrated Secco solution (15 min etching time). The resulting surface pits were imaged by a Zeiss Merlin scanning electron microscope (SEM) operated at 1.5 kV and the corresponding data were statistically analyzed using a freeware image analysis package.

The theoretical investigation of plastic relaxation in RG-VS SiGe layers was performed by means of a DD approach [25]. All the numerical simulations reported in the following were carried out by using the microMEGAs (mM) [26] DD code. In the DD approach, the evolution of a given

dislocation distribution is achieved by discretizing each dislocation line into small segments and evaluating the Peach-Kohler equation to obtain the driving force $\boldsymbol{F}$ acting on each of them:

$$\boldsymbol{F} = (\boldsymbol{\sigma} \cdot \boldsymbol{b}) \times \boldsymbol{\xi} \tag{1}$$

where $\boldsymbol{b}$ is the Burgers vector of the considered segment, $\boldsymbol{\xi}$ its line direction and $\boldsymbol{\sigma}$ is the local stress tensor acting at its position. The latter can be due to the self-interactions with other segments composing the same dislocation line, to the interactions with other dislocations and to external loads like the heteroepitaxial biaxial stress field. In mM, the stress field produced by the dislocation segments is evaluated by means of analytical expressions, as the ones reported by Hirth and Lothe in Ref. [27]. With this procedure, the evolution of the dislocation line can be modeled by the movement of all its composing segments following the driving force of equation (1) and eventually handling the possibility of local reactions between them. These topological reactions are evaluated whenever two segments during their motion cross each other and depending on the kind of the two interacting segments, the final results can be, for instance, the annihilation of the two segments or the formation of a junction between them.

The DD approach is applied here to study the relaxation of thin films and, thus, we exploited the capped-layer approach. As described by Schwarz [28], this approach permits to overcome the limitation of the classical DD approaches which rely on analytical expressions for the evaluation of the stress field produced by dislocation segments. Indeed, while the correct stress field of dislocations near free surfaces of a generic geometry can be obtained only by numerically tackling the partial differential equation of mechanical equilibrium [29, 30], e.g. by means of the Finite Element Method, the capped layer approach can be conveniently exploited for the particular case of thin films with a flat free surface. As shown by several studies [31-33], the error introduced by this approximation, e.g. on the evaluation of the critical strain for TD movement, is less than 5%.

This level of uncertainty is comparable to that introduced by the uncertainty of other parameters used in the linear elasticity defect theory, e.g. the cut-off radius to include the core energy of dislocations in a continuum framework, and, thus, does not affect significantly the expected overall level of accuracy of a DD simulation.

In this work, we applied the DD approach to study the relaxation of the heterostructures presented in this section. This was achieved by setting the initial condition of all the simulations by introducing a random distribution of TDs with an areal density matching the TDD experimentally observed for all the considered thickness of the Ge buffer layer. No further dislocation nucleation was considered. Following the experimental results, the heteroepitaxial strain of the Ge buffer layer is considered to be, on average, fully relaxed by a network of misfit dislocation, not directly modeled in our approach. The TDs that are present in the buffer layer are propagated into the top SiGe layer and are then let to evolve under the influence of the misfit strain in the RG top layer.

III. RESULTS AND DISCUSSION

In order to understand the dislocation dynamics in our material system, we first investigate the evolution of the TDD as a function of the thickness of relaxed Ge layers.

In Fig. 1, we display the results of the TDD count obtained on samples featuring a Ge thickness up to 7.8 μm. Remarkably, all the investigated samples were crack-free, despite the large bowing, due to the thermal strain accumulated during the growth owing to the different coefficient of thermal expansion of the Ge epi-layer and the Si substrate [34, 35]. Furthermore, we would like to mention here that, even for Ge thickness up to 7.8 μm, all grown Ge/Si(001) VSs exhibit a rms roughness value < 1 nm (~ 0.8 – 0.3 nm). As an exemplary case, we show in the inset of Fig. 1 a (10×10) μm² AFM image of a 2.3 μm-thick Ge/Si(001) layer, showing the characteristic cross-

hatch pattern and a rms roughness value of 0.44 nm, in agreement with previous literature reports [2, 5].

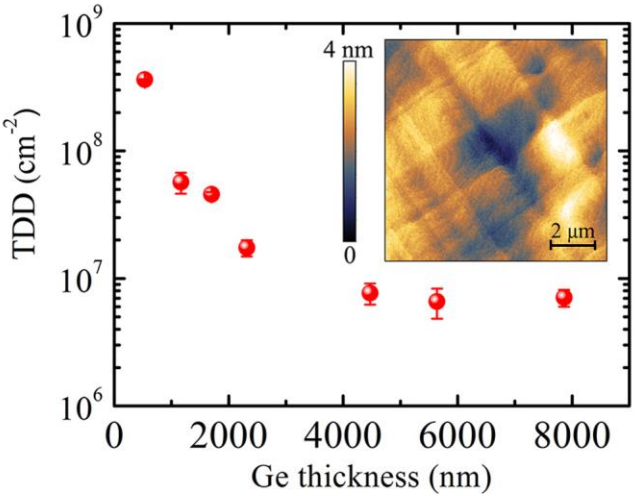

Figure 1: TDD as a function of Ge thickness in Ge/Si(001) samples. The inset shows an exemplary (10x10) µm² AFM image of the sample with 2.3 µm of Ge. Next to the AFM image, the corresponding vertical scale bar is reported. The rms roughness value obtained from the image is 0.44 nm.

By analyzing in detail Fig. 1, we note that, initially, the TDD decreases fast with increasing Ge thickness, showing an almost two-decade reduction for a Ge layer thickness of ~2.5 – 3 µm. A further increase of the epi-layer thickness leads nearly to a saturation of the TDD which reaches a saturation value of 7×10^6 cm^{-2}.

The reduction of TDD for increasing thickness of a fully relaxed epi-layer is commonly reported in literature [2, 20, 23] and it is interpreted within the "geometrical model" [36]. As the system is fully relaxed, the extension of existing misfit segments is hindered and the only driving force for TD motion is the interaction with other TDs, possibly leading to their mutual annihilation when TDs featuring opposite Burger's vector are close enough. By increasing Ge layer thickness, since the dislocations glide on {111} planes, the probability of two TDs approaching each other is increased and, thus, their annihilation enhanced. However, the probability of an annihilation event

is progressively reduced for decreasing TDD and the geometrical effect is gradually less important, thus explaining the observed saturation behavior.

As a subsequent step, we investigated how the plastic relaxation occurs and the TDD evolves if a second epi-layer, made of a Ge-rich $Si_{0.06}Ge_{0.94}$ alloy, is deposited on top of Ge/Si heterostructures, now acting as a VS. In order to understand how the presence of an upper layer of reduced Ge content affects the TDD, we first realized a series comprising samples made of a $Si_{0.06}Ge_{0.94}$ layer of variable thickness t_{SiGe} = [250 nm – 1.2 µm] on a 1.2 µm Ge/Si(001) substrate. This corresponds to a total thickness of the heterostructures up to 2.4 µm, i.e. close to the thickness at which we observed the onset of the TDD saturation in the case of Ge/Si(001) layers (see. Fig.1). As described in Section II, the TDDs of all samples were measured using the etch pit count method based on the Secco etch. As an exemplary image, we show in Fig. 2(a) the SEM picture of the surface of the thickest sample of this series (1.2 µm $Si_{0.06}Ge_{0.94}$/1.2 µm Ge/Si(001) sample). To demonstrate that the rms roughness is not worsened with respect to a Ge/Si(001) VS of the same total thickness, we show, in Fig. 2(b), a (10 x 10) µm² AFM image of the 1.2 µm $Si_{0.06}Ge_{0.94}$/1.2 µm Ge/Si(001) sample. The corresponding rms roughness value measured on the image is 0.41 nm, matching well that reported in Fig. 1 for a 2.3 µm Ge/Si(001) sample (0.44 nm). We can then see that the introduction of a $Si_{0.06}Ge_{0.94}$ layer has very limited impact on the surface roughness.

In Fig. 2(c), we show the corresponding XRD reciprocal space mapping (RSM) around the $(\bar{2}\bar{2}4)$ reflections of SiGe and Ge. We can clearly see that the Ge layer features a slight over-relaxation, with a residual tensile strain $\varepsilon \sim 2\times10^{-3}$, corresponding to a relaxation value respect the Si substrate of $R \sim 105$ %.

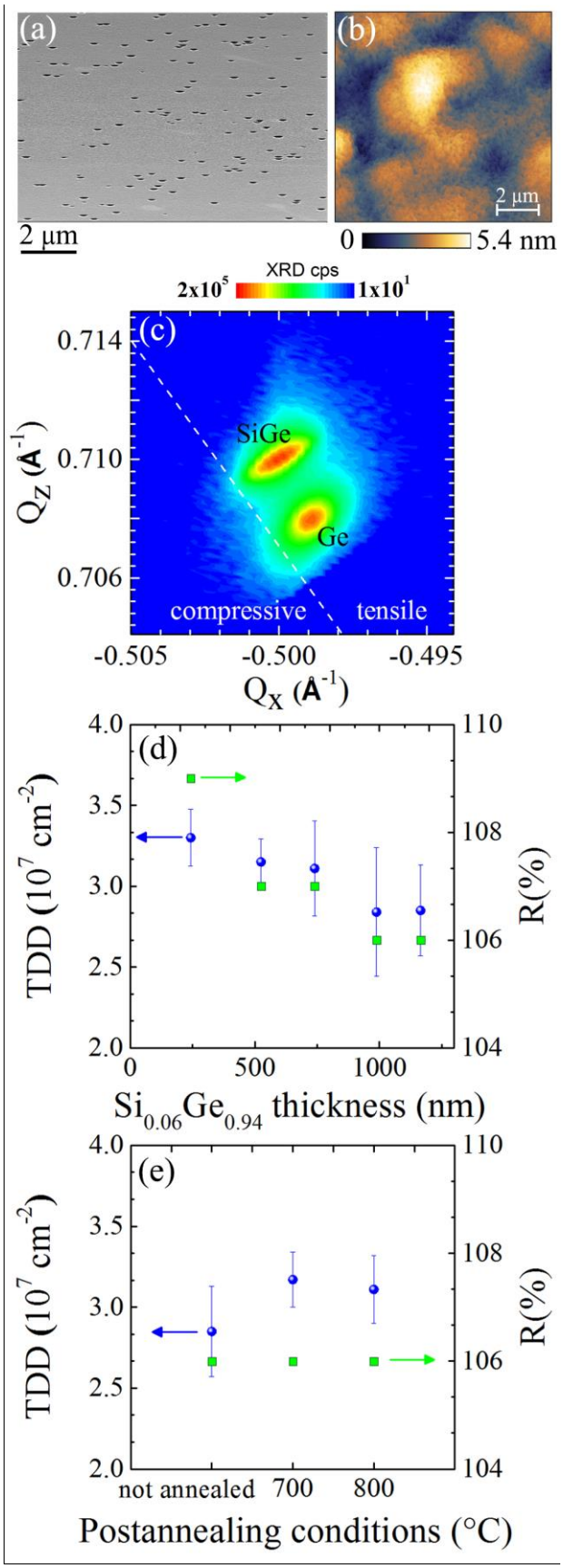
(a)
2 μm
(b)
2 μm
0
5.4 nm
XRD cps
2x10^5
1x10^1
(c)
SiGe
Ge
compressive
tensile
0.714
0.710
0.706
Q_Z (Å^-1)
-0.505
-0.500
-0.495
Q_X (Å^-1)
(d)
TDD (10^7 cm^-2)
R(%)
4.0
3.5
3.0
2.5
2.0
110
108
106
104
0
500
1000
Si0.06Ge0.94 thickness (nm)
(e)
TDD (10^7 cm^-2)
R(%)
not annealed
700
800
Postannealing conditions (°C)

Figure 2: (a) SEM image of the 1.2 µm $Si_{0.06}Ge_{0.94}$/1.2 µm Ge/Si(001) sample after 15 min Secco etch: etch pits are clearly visible. (b) (10x10) µm² AFM image of the same sample as in (a). The vertical scale bar is displayed below the image on which a rms roughness value of 0.41 nm is measured. (c) XRD RSM of the asymmetric $(\bar{2}\bar{2}4)$ reflections of SiGe and Ge measured on the same sample. Q_z-axis is parallel to the [001] direction while Q_x-axis is oriented along the $[\bar{1}\bar{1}0]$. (d) TDD (blue dots) and relaxation degree *R* (green squares) as a function of the thickness of $Si_{0.06}Ge_{0.94}$ films grown on 1.2 µm Ge/Si(001). (e) TDD and *R* values obtained for different postannealing processes on the 1.2 µm $Si_{0.06}Ge_{0.94}$/1.2 µm Ge/Si(001) sample.

The peak position corresponding to the SiGe signal has been used to determine the degree of relaxation *R* of the top-layer reported in Fig. 2(d) (green squares) together with the corresponding TDD (blue dots). For increasing $Si_{0.06}Ge_{0.94}$ thickness, we observed a slight decrease of the relaxation up to a t_{SiGe} = 1 µm, saturating afterwards at a value *R* = 106 %, indicating the attainment of the maximum relaxation of the epitaxial strain. The TDD evolves in a similar manner, featuring a mild decrease from 3.3×10^7 cm^{-2} down to 2.7×10^7 cm^{-2} . We verified that the absence of any kinetic limitation to the relaxation nor to the TDD mobility (and consequently to the probability of their annihilation) by annealing the samples at temperatures higher than the growth temperature. To this end, two identical, fully relaxed 1.2 µm $Si_{0.06}Ge_{0.94}$/1.2 µm Ge/Si(001) samples were post-annealed at different temperatures (700 and 800 °C for 10 min). The *R* and the corresponding TDD values are plotted in Fig. 2(e). It is worth noting that the post-annealing process did not affect, within the experimental error, the relaxation nor the TDD. Upon comparing these data with the Ge/Si sample having the same total thickness, we note that the $Si_{0.06}Ge_{0.94}$ layer relaxation reaches a saturation value *R* = 106 %, slightly larger than what was observed for the Ge/Si layers (*R* = 105%). While, in principle, the same *R* value should be expected for the two cases, since the coefficients of thermal expansion of Ge and $Si_{0.06}Ge_{0.94}$ are practically equal and the thermal budget used in the growth is also identical, the slightly larger value of *R* observed for the $Si_{0.06}Ge_{0.94}$/Ge/Si(001) sample can be attributed to the hardening effect, hindering the complete

relaxation of the second epilayer [35]. Thus, we can conclude that a 1.2 µm $Si_{0.06}Ge_{0.94}$ layer added on top of a 1.2 µm Ge/Si(001) heterostructure results in a fully relaxed RG-VS, with no remaining driving force for TD motion. The resulting TDD is a factor 2× larger to that measured in the case of Ge/Si.

Based on these findings, two questions arise: Why is this happening and, more generally, what is the impact of the TDs already developed in the Ge/Si layer for the relaxation process of the tensile strained $Si_{0.06}Ge_{0.94}$ /Ge layer?

In the following, we aim at addressing these puzzling questions.

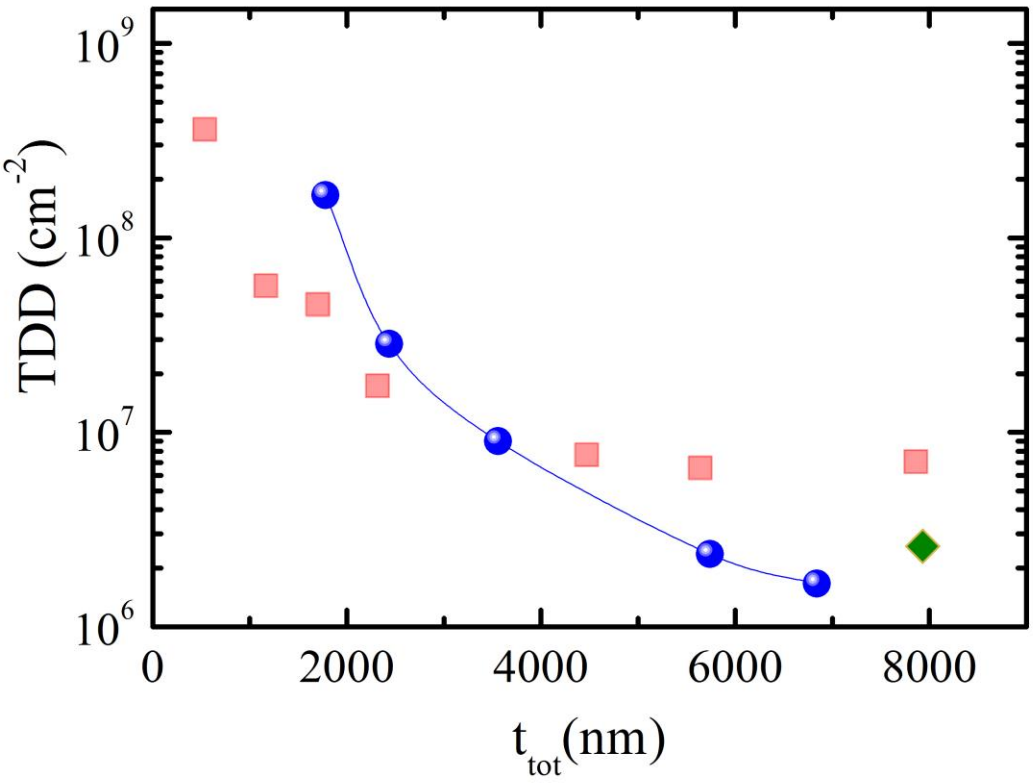

Figure 3: TDD as a function of the heterostructure thickness t_{tot} (obtained by varying only the Ge layer thickness) for Ge/Si(001) samples (semi-transparent red squares) and for 1.2 µm $Si_{0.06}Ge_{0.94}$/Ge/Si(001) samples (blue dots). The green diamond marker corresponds to a double Ge/SiGe interface featuring the following module structure: 1.2 µm Ge/1.2 µm $Si_{0.06}Ge_{0.94}$/Ge/Si(001) (see text).

To this purpose, we realized a sample series by depositing identical 1.2 µm $Si_{0.06}Ge_{0.94}$ layers on Ge/Si VS featuring five different thicknesses and consequently, as shown in Fig. 1 and previously discussed, different TDDs. All the $Si_{0.06}Ge_{0.94}$ show the same value of the strain relaxation R= 106 % (not shown) and a decreasing TDD value, as depicted in Fig. 3 (blue dots). Taking as a reference the preexisting TD population in Ge/Si(001) samples (semi-transparent red squares), we can observe that the drop of TDD with the total heterostructures thickness t_{tot} = $t(Si_{0.06}Ge_{0.94})$ + t(Ge) is more rapid for the $Si_{0.06}Ge_{0.94}$/Ge/Si(001) than for the Ge/Si(001) VS. As such, for t_{tot} < 3 µm, the $Si_{0.06}Ge_{0.94}$/Ge/Si(001) samples have a larger TDD than Ge/Si samples, while the opposite holds for the region t_{tot} >3 µm, where we observed the saturation by the geometrical effect. We point out here that the lowest TDD achieved reaches the remarkable value of 1.7×10^6 cm^{-2}, for t_{tot} ~7 µm, being a factor 4× lower than the corresponding value for a Ge/Si VS of similar thickness. Importantly, by growing an additional sample featuring another 1.2 µm 100% Ge film on top of such heterostructure and inserting in this way another heterointerface, the TDD is found to be 2.5×10^6 cm^{-2}. This value is in-line with the one obtained in the $Si_{0.06}Ge_{0.94}$/Ge/Si(001) heterostructures and thus still well below the saturation limit for the geometrical effect in Ge/Si(001) (green diamond in Fig. 3). Therefore, this approach represents a viable path to obtain fully relaxed Ge layers featuring a lower TDD at equal total thickness.

Having previously shown that a 1.2 µm-thick SiGe/Ge/Si layer is stable against any reduction of the TDD during annealing cycles (see Fig. 2(d)), this result clearly points to a pivotal role of the $Si_{0.06}Ge_{0.94}$/Ge heterointerface on the TDD evolution.

To shed light on this behavior, we performed some dedicated DD simulations and an additional cross-section TEM characterization.

The effect produced by the introduction of a RG layer at high heterostructure thickness can be appreciated by looking at the simulation results reported in Fig. 4. Here, the simulation parameters were set in order to match the samples analyzed in Fig. 3. In particular, a 4.5 μm Ge buffer layer was considered with a 1.2 μm top layer consisting of pure Ge [Fig. 4(a)] or $Si_{0.06}Ge_{0.94}$ [Fig. 4(b)]. As explained in Section II, our simulation approach consists in setting the initial areal density of TDs in order to match the values reported in Fig. 3 for the corresponding Ge buffer thickness (TDD of about 8×10^6 cm^{-2} for the case under consideration). In Fig. 4(a), one can observe how these TDs evolve only marginally over time, with no annihilation events taking place due to the low probability of TDs encountering at this low TDD value. This is precisely what is expected to occur once the saturation limit, clearly visible in Fig.1, is reached and the geometric effect ceases to be effective [36]. On the contrary, the addition of a strained SiGe RG layer as in Fig. 4(b) provides additional mobility to the TDs, bending them at the new interface in order to release the excess strain in the top layer and enhancing the probability of annihilation. We actually verified that, during the evolution depicted in Fig. 4(b), bending of pre-existing threading arms results in nearly full strain relaxation of the upper layer. With this respect, there is no need to invoke further nucleation of dislocations to explain the experimentally observed relaxation of the $Si_{0.06}Ge_{0.94}$ layer. The resulting TDD evolution for the two simulated cases is reported in Fig. 4(c).

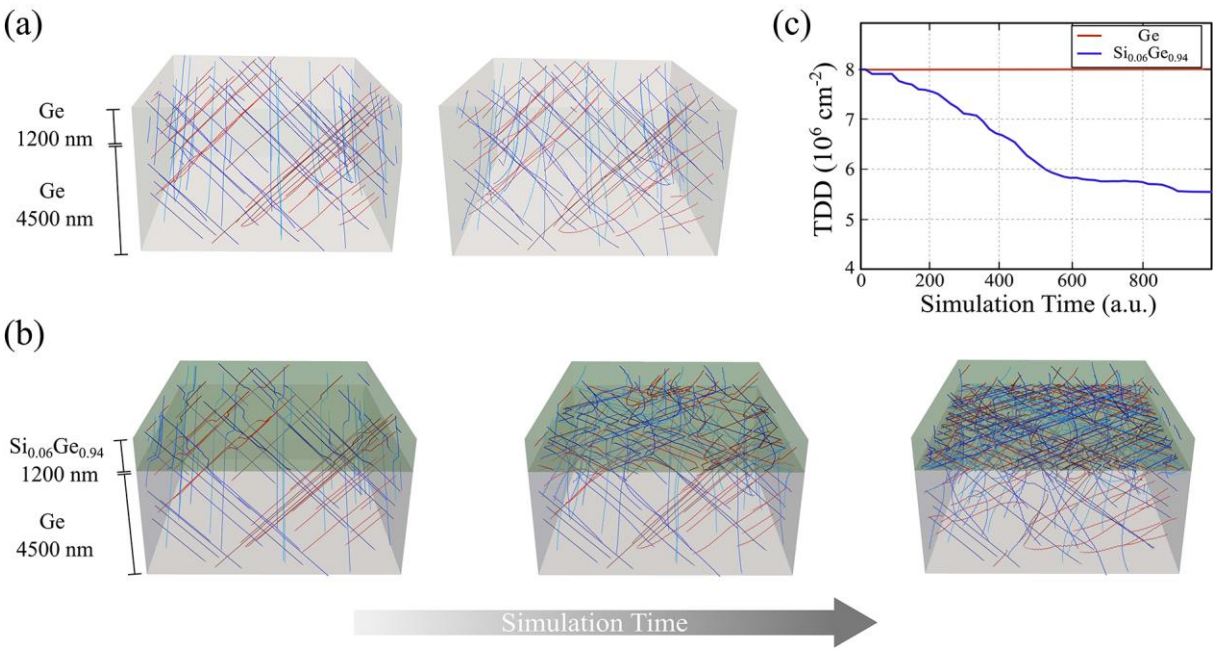

Figure 4: Simulated images obtained from Dislocation Dynamics Simulations depicting TD motion over time in heterostructures consisting of 1.2 µm-thick (a) Ge and (b) $Si_{0.06}Ge_{0.94}$ on top of 4.5 µm-thick Ge/Si(001) VS. (c) Behaviour of TDD as a function of the simulation time for the heterostructures in (a) (red curve) and (b) (blue curve).

Based on the insights on TDs behavior we obtained, we can propose the following scenario.

At high heterostructure thickness (> 3 µm), when the "geometric" process has reached its saturation, so that increasing the thickness of the Ge buffer layer produces a negligible probability of interaction between the remaining TDs [36], the deposition of a top layer of different composition and lattice parameter (like $Si_{0.06}Ge_{0.94}$) can provide an alternative mechanism to TDD reduction. Indeed, the additional strained layer needs to be plastically relaxed. To do so, instead of nucleating new dislocations surmounting the associated kinetic barrier, it is easier to exploit pre-existing TDs. This requires "bending" them at the additional heterointerface to develop a new network of misfit segments [37]. This re-established dislocation mobility can favor again the annihilation of TDs and, consequently, be responsible of the observed decrease of TDD. With this respect, the RG layer effectively acts like a "filtering layer" [38]. On the other thickness limit (< 3

μm), the introduction of the $Si_{0.06}Ge_{0.94}$/Ge RG interface is found to be detrimental for the action of the geometric effect, because bending the TDs effectively lowers the layer thickness where they can encounter each other and annihilate.

The above described bending mechanism can be better appreciated by looking at Fig. 5, where we display an additional TEM analysis based on lamellas taken out of two selected heterostructure samples, consisting of 0.5 μm Ge (Fig. 5(a)) and 0.5 μm $Si_{0.06}Ge_{0.94}$ (Fig. 5(b)) on 1.2 μm Ge/Si(001) VS. From the cross-section STEM images, it can be seen that, for the same total thickness of the layers, the pure-Ge sample exhibits TDs running through the whole heterostructure, reaching also the upper layer (Fig. 5(a)). On the contrary, for the sample featuring the $Si_{0.06}Ge_{0.94}$/Ge RG heterointerface displayed in Fig. 5(b), an increased contrast of the heterointerface can be observed, due to the higher MD density required for accommodating the lattice mismatch during the plastic relaxation of the $Si_{0.06}Ge_{0.94}$ layer. Two exemplary STEM images of the heterointerface are seen in Figs. 5(c) and 5(d). In Fig. 5(c), a TD arm along the heterointerface is bending into the Ge buffer layer (red arrow mark) after encountering a MD. In Fig. 5(d), a TD arm coming from the Ge layer is "captured" at the heterointerface, where we observe the presence of the MDs needed to plastically relax the SiGe top layer. We point out that that some of these MDs may originate from the bending of other TDs coming from the Ge layer.

In Figs. 5(e) and 5 (f), we show simulated TEM images obtained by properly sectioning the simulation cells at the final stage of DD simulations. These were performed in order to reproduce the samples analyzed in the TEM images of Fig 5(a) and (b) with, respectively, 0.5 μm-thick Ge and $Si_{0.06}Ge_{0.94}$ on top of 1.2 μm-thick Ge/Si(001). In the pure-Ge case (Fig. 5(f)), the simulation shows TDs running unhindered through the whole heterostructure, also reaching the upper Ge layer. On the contrary, Figure 5(e) shows a totally different scenario, with the formation of a

second dislocation network at the new Ge/SiGe interface due to the bending of TDs, relaxing the strain of the top layer. It is safe to state that the DD simulated TEM images match well the experimental TEM images.

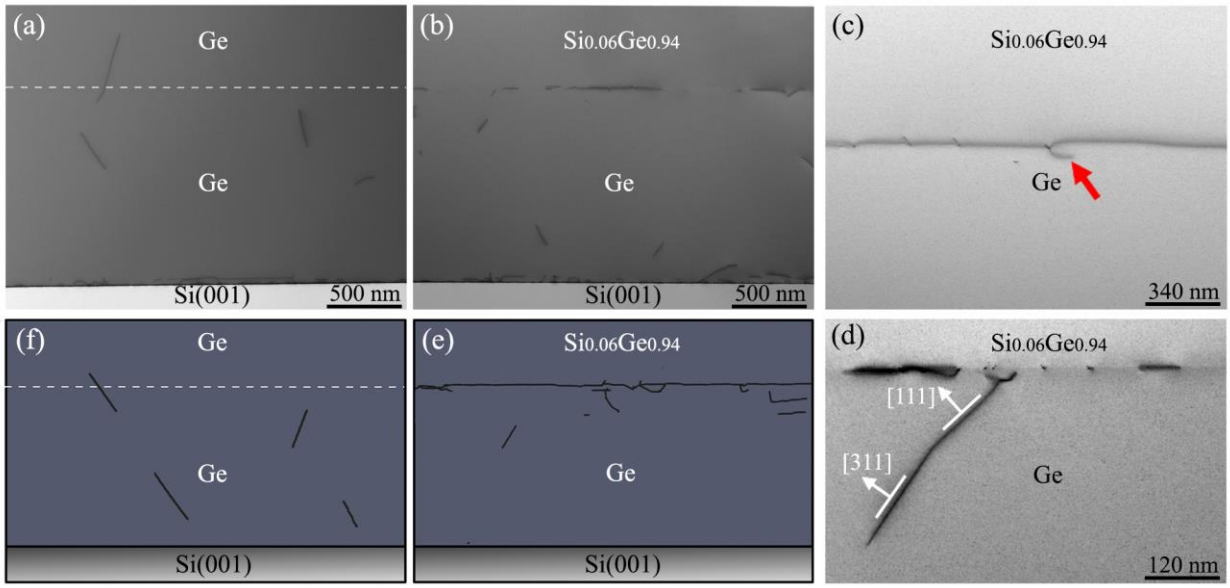

Figure 5: STEM images of samples featuring a 1.2 µm-thick Ge/Si(001) stack on top of which a 0.5 µm-thick layer of (a) Ge and (b) $Si_{0.06}Ge_{0.94}$ are deposited. In panels (c)-(d), STEM images of the $Si_{0.06}Ge_{0.94}$/Ge interface are shown, evidencing (c) a TD arm along the heterointerface (marked by the red arrow) which "bends" into the Ge buffer layer and (d) the effect of a TD arm meeting a MD at the heterointerface. Simulated TEM images based on DD simulations corresponding to 0.5 µm-thick (e) $Si_{0.06}Ge_{0.94}$ and (f) Ge layer on top of 1.2 µm-thick Ge/Si(001).

IV. CONCLUSIONS

In this paper, we have proposed and quantitatively analyzed a strategy to lower the TDD in both tensile films grown on Ge/Si(001) and Ge films grown on Si(001).

After having established a saturation limit for the TDD in Ge/Si(001) films grown by our RPCVD reactor (~ 7×10^6 cm^{-2} for our growth procedure), we explored the possibility to achieve a further reduction of TDD by $Si_{0.06}Ge_{0.94}$/Ge/Si(001) RG-VS. This proved to be possible only when the TDD in the Ge/Si(001) film underneath was sufficiently low. Under these conditions,

dislocation annihilation by the simple geometrical effect ceases to take place, while bending and gliding of threading arms at the $Si_{0.06}Ge_{0.94}$/Ge interface promote further interaction and annihilation, as directly shown by DD simulations. By proper tuning of the growth parameters, we were able to reach a very low TDD value of ~ 1.7×10^6 cm^{-2}. Very interestingly, when a low TDD is reached in $Si_{0.06}Ge_{0.94}$/Ge/Si(001) RG-VS, an overgrown Ge film displays a TDD being much lower than the Ge/Si(001) saturation limit. We therefore believe that the present methodology can be extremely useful in achieving low TDDs also in 100% Ge films, without the need to use neither continuous grading nor etching-back procedures.

ACKNOWLEDGMENTS

This project was funded by the European Union's Horizon 2020 research and innovation program under Grant Agreement No. 766719 (FLASH).

REFERENCES

[1] K. Wada and L.C. Kimerling, Photonics and Electronics with Germanium, Book XVI, 2015, Wiley-VCH, New York.

[2] Y. Yamamoto, P. Zaumseil, M. A. Schubert, and B. Tillack, Semicond. Sci. Technol. **33**, 124007 (2018).

[3] P. Hashemi, T. Ando, E.A. Cartier, J. Bruley, C.-H. Lee, and V. Narayanan, ECS Transactions **87**(7), 51 (2018).

[4] F.T. Armand Pilon, A. Lyasota, Y.-M. Niquet, V. Reboud, V. Calvo, N. Pauc, J. Widiez, C. Bonzon, J.M. Hartmann, A. Chelnokov, J. Faist, and H. Sigg, Nat. Commun. **10**, 2724 (2019).

[5] G. Capellini, M. De Seta, Y. Busby, M. Pea, F. Evangelisti, G. Nicotra, C. Spinella, M. Nardone, and C. Ferrari, J. Appl. Phys. **107**, 063504 (2010).

[6] S. Lischke, D. Knoll, L. Zimmermann, Y. Yamamoto, M. Fraschke, A. Trusch, A. Krüger, M. Kroh, and B. Tillack, Proc. IEEE Photonics Conference (IPC) **2012**, 628 (2012).

[7] D. Chen, Q. Guo, N. Zhang, A. Xu, B. Wang, Y. Li, and G. Wang, Mater. Res. Express **4**, 076407 (2017).

[8] M. Akie, T. Fujisawa, T. Sato, M. Arai, and K. Saitoh, IEEE J. Sel. Top. Quantum Electron. **24**, 1 (2018).

[9] M. Myronov, X.-C. Liu, A. Dobbie, and D.R. Leadley, J. Cryst. Growth **318**, 337 (2011).

[10] N.W. Hendrickx, D.P. Franke, A. Sammak, M. Kouwenhoven, D. Sabbagh, L. Yeoh, R. Li, M.L.V. Tagliaferri, M. Virgilio, G. Capellini, G. Scappucci, and M. Veldhorst, Nat. Commun. **9**, 2835 (2018).

[11] N.W. Hendrickx, D.P. Franke, A. Sammak, G. Scappucci, and M. Veldhorst, Nature **577**, 48 (2020).

[12] T. Grange, D. Stark, G. Scalari, J. Faist, L. Persichetti, L. Di Gaspare, M. De Seta, M. Ortolani, D.J. Paul, G. Capellini, S. Birner, and M. Virgilio, Appl. Phys. Lett. **114**, 111102 (2019).

[13] J.E. Halpin, S.D. Rhead, A.M. Sanchez, M. Myronov, and D.R. Leadley, Semicond. Sci. Technol. **30**, 114009 (2015).

[14] Y.B. Bolkhovityanov, A.S. Deryabin, A.K. Gutakovskii, and L. V. Sokolov, J. Appl. Phys. **109**, 123519 (2011).

[15] A. Marzegalli, M. Brunetto, F. Montalenti, G. Nicotra, M. Scuderi, C. Spinella, M. De Seta, and G. Capellini, Phys. Rev. B **88**, 165418 (2013).

[16] E.A. Fitzgerald, Mater. Sci. Rep. **7**(3), 87 (1991).

[17] E.A. Fitzgerald, Y.-H. Xie, M.L. Green, D. Brasen, A.R.Kortan, J. Michel, Y.-J. Mii, and B.E. Weir, Appl. Phys. Lett. **59**(7), 811 (1991).

[18] J. Tersoff, Appl. Phys. Lett. **62**, 693 (1993).

[19] J. Zhang, X. Chen, J.A. Wang, G.B. Chen, Z.H. Tang, K.Z. Tan, and W. Cui, IOP Conf. Series: Materials Science and Engineering **504**, 012020 (2019).

[20] V.A. Shah, A. Dobbie, M. Myronov, and D.R. Leadley, J. Appl. Phys. **107**, 064304 (2010).

[21] V.A. Shah, A. Dobbie, M. Myronov, D.J.F. Fulgoni, L.J. Nash, and D.R. Leadley, Appl. Phys. Lett. **93**, 192103 (2008).

[22] K. Gallacher, M. Ortolani, K. Rew, C. Ciano, L. Baldassarre, M. Virgilio, G. Scalari, J. Faist, L. Di Gaspare, M. De Seta, G. Capellini, T. Grange, S. Birner, and D.J. Paul, Opt. Express **28**, 4786 (2020).

[23] Y. Yamamoto, P. Zaumseil, T. Arguirov, M. Kittler, and B. Tillack, Solid-State Electron. **60**, 2 (2011).

[24] J.P. Dismukes, L. Ekstrom, R.J. Pfaff, J. Phys. Chem. **68**, 3021 (1964).

[25] L.P. Kubin, Dislocations, mesoscopic simulations and plastic flow, Oxford Series on Materials Modelling, 2013, Oxford University Press, Oxford.

[26] B. Devincre, R. Madec, G. Monnet, S. Queyreau, R. Gatti, and K. Ladislas, Modeling crystal plasticity with dislocation dynamics simulations: the ‘microMegas’ code, Collection Sciences de la matière, 2011, Presses des l'Ecole des Mines, Paris.

[27] J. Hirth and J. Lothe, Theory of Dislocations, 1982, Krieger Publishing, Malabar.

[28] K. Schwarz, J. Appl. Phys. **85**, 108 (1999).

[29] O. Jamond, R. Gatti, A. Roos, and B. Devincre, International Journal of Plasticity **80**, 19 (2016).

[30] F. Rovaris, F. Isa, R. Gatti, A. Jung, G. Isella, F. Montalenti, and H. von Kaenel, Phys. Rev. Materials **1**, 073602 (2017).

[31] L. Freund, J. Appl. Mech. **54**, 553 (1987).

[32] K. Schwarz, J. Cai, and P. M. Mooney, Appl. Phys. Lett. **85**, 2238 (2004).

[33] K. Schwarz, Model. Simul. Mater. Sci. Eng. **11**, 609 (2003).

[34] C.L. Manganelli, M. Virgilio, O. Skibitzki, M. Salvalaglio, D. Spirito, P. Zaumseil, Y. Yamamoto, M. Montanari, W.M. Klesse, and G. Capellini, J. Raman Spectrosc. **2020**, 1 (2020).

[35] G. Capellini, M. De Seta, P. Zaumseil, G. Kozlowski, and T. Schroeder, J. Appl. Phys. **111**, 073518 (2012).

[36] A.E. Romanov, W. Pompe, G. Beltz and J.S. Speck, Phys. Status Solidi (b) **198**, 599 (1996).

[37] B.W. Dodson, J. Elect. Mater **19**, 503 (1990).

[38] T. Ward, A.M. Sánchez, M. Tang, J. Wu, H. Liu, D.J. Dunstan, and R. Beanland, J. Appl. Phys. **116**, 063508 (2014).